COMPDYN 2011
III ECCOMAS Thematic Conference on
Computational Methods in Structural Dynamics and Earthquake Engineering
M. Papadrakakis, M. Fragiadakis, V. Plevris (eds.)
Corfu, Greece, 25–28 May 2011

AN EFFICIENT *H*-ADAPTIVE SCALED BOUNDARY ELEMENT METHOD FOR TRANSIENT ELASTODYNAMICS

Zihua Zhang[1], Zhenjun Yang[2]*, Guohua Liu[1], Yunjin Hu[1]

[1]College of Civil Engineering and Architecture, Zhejiang University
Hangzhou, 310058, China
zhangzihua1984@googlemail.com

[2*]School of Engineering, the University of Liverpool
Brownlow Street, Liverpool, L69 3GQ, UK
zjyang@liv.ac.uk

Keywords: Scaled boundary finite element method, *h*-hierarchical adaptivity, subdivision of subdomains, mesh mapping, elastodynamics

Abstract. *This study develops a posterior h-hierarchical adaptive scaled boundary finite element method for transient elastodynamic problems using a mesh refinement procedure which subdivides subdomains. In a time step, the fields of displacement, stress, velocity and acceleration are all semi-analytical and the kinetic energy, strain energy and energy errors are all semi-analytically integrated in subdomains. This makes mesh mapping very simple but accurate. Mesh refinement is very simple, flexible and efficient because only a small number of subdomains are subdivided due to the high accuracy of the SBFEM. The results of an example with stress wave propagation were presented. It is shown that the developed method is capable of capturing the propagation of steep stress regions and calculating accurate dynamic responses, but only using a fraction of degrees of freedom required by adaptive finite element methods.*

1 INTRODUCTION

A few adaptive spatial discretisation methods based on finite element method (FEM) and *posteriori* error estimators have been developed to efficiently simulate elastodynamic problems with stress wave propagation [1, 2]. However, there still exist two major difficulties in adaptive finite element method (AFEM). First, automatic remeshing to capture the stress wave propagation usually involves complicated and time-consuming topological changes on a large number of small-sized elements, especially for large-scale problems. This may also lead to ill-shaped elements resulting in inaccurate responses. Second, mesh mapping after remeshing to transfer state variables from the old mesh to the new one is approximate, which may lead to high accumulative errors in later time steps. In addition, identifying the old element where a new node is located may be time-consuming as well because a large number of finite elements need to be checked.

The scaled boundary finite element method (SBFEM) developed in 1990s [3, 4] is a semi-analytical method combining the advantages of the FEM and the boundary element method (BEM). It models an analysis domain by a small number of large-sized subdomains and only the subdomain boundaries are discretised, and the modeled dimensions are reduced by one as the BEM, but no fundamental solutions or singular integrations are needed. Therefore, the FEM's wide applicability and the BEM's simplicity in remeshing are both retained.

This study aims to further extend the applicability of the SBFEM by developing an adaptive SBFEM (ASBFEM) for transient elastodynamic problems using a simple subdomain subdivision procedure. A simply-supported beam under impact was modeled to validate the developed ASBFEM.

2 METHODOLOGY

2.1 The scaled boundary finite element method

A domain of analysis is illustrated in Figure 1(a) as an example. The domain is divided into three subdomains whose geometry and dimensions are defined by a few vertices. Figure 1(b) shows the details of Subdomain 1. The subdomain is represented by scaling a defining curve S relative to a scaling centre. A normalized radial coordinate ξ is defined, varying from zero at the scaling centre and unit value on S. A circumferential coordinate η is defined around the defining curve S. A curve similar to S defined by ξ=0.5 is shown in Figure 1b. The coordinates ξ and η form a local coordinate system used in all the subdomains and simple transformation equations between the local and global coordinates can be identified with ease for each subdomain:

$$x = x_0 + \xi\left(\frac{x_1 + x_2 - 2x_0}{2} + \frac{(x_2 - x_1)\eta}{2}\right) \tag{1}$$

$$y = y_0 + \xi\left(\frac{y_1 + y_2 - 2y_0}{2} + \frac{(y_2 - y_1)\eta}{2}\right) \tag{2}$$

where (x_1, y_1) and (x_2, y_2) are nodal coordinates of a two-node element on the boundary and (x_0, y_0) are the coordinates of the scaling centre. The displacements of any point (ξ, η) in a subdomain are assumed as

$$\mathbf{u}(\xi, \eta) = \mathbf{N}(\eta)\mathbf{u}(\xi) \tag{3}$$

where $\mathbf{u}(\xi)$ are the displacements along the radial lines and are analytical with respect to ξ. $\mathbf{N}(\eta)$ is the shape function matrix in the circumferential direction.

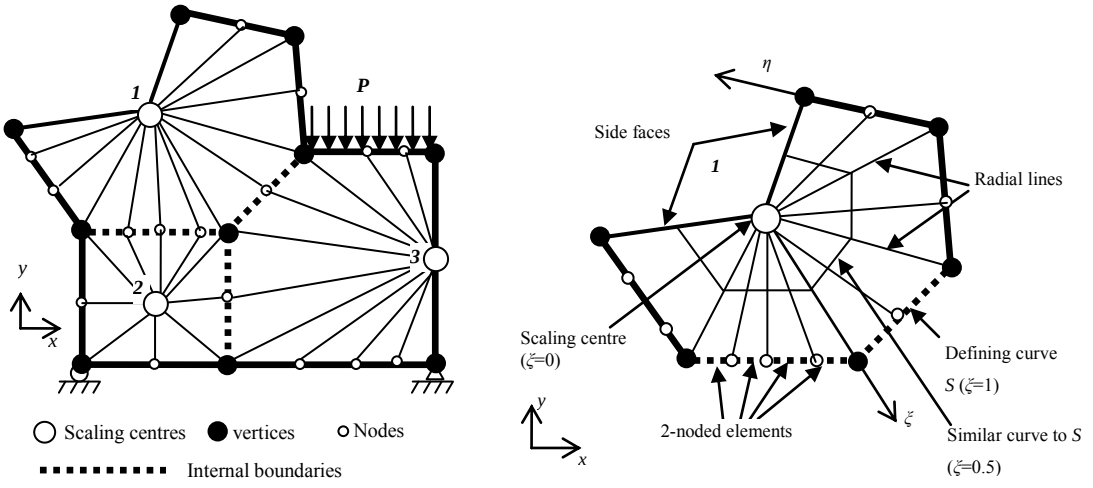

(a) Subdomaining of a domain (b) Subdomain 1

Figure 1 The concept of the scaled boundary finite element method

For linear elastic materials, the stress vector in a subdomain is calculated by

$$\boldsymbol{\sigma}(\xi,\eta)=\mathbf{D}\mathbf{B}^{1}(\eta)\mathbf{u}(\xi),_{\xi}+\frac{1}{\xi}\mathbf{D}\mathbf{B}^{2}(\eta)\mathbf{u}(\xi) \tag{4}$$

where $\mathbf{B}^1(\eta)$ and $\mathbf{B}^2(\eta)$ are coefficient matrixes, and $\mathbf{D}$ is the elasticity matrix.

2.2 Solutions in time domain

In elastodynamics, the dynamic equilibrium equation of a subdomain is derived as [5]

$$\mathbf{M}_s\ddot{\mathbf{u}}_\mathbf{b}+\mathbf{K}_s\mathbf{u}_\mathbf{b}=\mathbf{p}_s \tag{5}$$

where $\mathbf{u}_b$ is the displacement vector and $\ddot{\mathbf{u}}_b$ is the acceleration vector on the subdomain boundary, $\mathbf{p}_s$ the subdomain load vector, $\mathbf{K}_s$ the subdomain stiffness matrix and $\mathbf{M}_s$ the subdomain mass matrix.

Assembling Eq. (5) for all subdomains lead to the global equation system

$$\mathbf{M}\ddot{\mathbf{U}}+\mathbf{K}\mathbf{U}=\mathbf{P} \tag{6}$$

where $\mathbf{M}$ and $\mathbf{K}$ are the assembled global mass and stiffness matrices, $\mathbf{P}$ is the global load vector, $\mathbf{U}$ and $\ddot{\mathbf{U}}$ are the nodal displacement and acceleration vectors respectively.

The Newmark integration scheme [6] is used to solve Eq. (6). At time step n, the state variables are calculated by

$$(a_1\mathbf{M}+\mathbf{K})\mathbf{U}_n=\mathbf{F}_n+\mathbf{M}(a_1\mathbf{U}_{n-1}+a_2\dot{\mathbf{U}}_{n-1}+a_3\ddot{\mathbf{U}}_{n-1}) \tag{7a}$$

$$\ddot{\mathbf{U}}_n=a_1(\mathbf{U}_{n-1}-\mathbf{U}_{n-1})-a_2\dot{\mathbf{U}}_{n-1}-a_3\ddot{\mathbf{U}}_{n-1} \tag{7b}$$

$$\dot{\mathbf{U}}_n=\dot{\mathbf{U}}_{n-1}+a_4\ddot{\mathbf{U}}_{n-1}+a_5\ddot{\mathbf{U}}_n \tag{7c}$$

$$a_1=\frac{1}{\beta(\Delta t)^2},\quad a_2=\frac{1}{\beta\Delta t},\quad a_3=\frac{1}{2\beta}-1,\quad a_4=\Delta t(1-\gamma),\quad a_5=\gamma\Delta t \tag{8}$$

where Δt is the time increment, β and γ are the Newmark parameters. In this study, $\beta = 0.25$ and $\gamma = 0.5$ are used for all the examples with unconditional stability.

The subdomain displacement and stress field are

$$\mathbf{u}(\xi,\eta)=\mathbf{N}(\eta)\sum_{i=1}^{N}c_i\xi^{\lambda_i}\boldsymbol{\varphi}_i \tag{9}$$

$$\boldsymbol{\sigma}(\xi,\eta)=\mathbf{DB}^{1}(\eta)\left(\sum_{i=1}^{N}c_i\lambda_i\xi^{\lambda_i-1}\boldsymbol{\varphi}_i\right)+\mathbf{DB}^{2}(\eta)\left(\sum_{i=1}^{N}c_i\xi^{\lambda_i-1}\boldsymbol{\varphi}_i\right) \tag{10}$$

where λ_i and $\boldsymbol{\varphi}_i$ (i=1-N) are eigen values and eigen vectors from solving a standard eigen problems [7]. $\mathbf{c}=\{c_1, c_2, \ldots, c_N\}^T$ are constants dependent on boundary conditions, and N is the number of degrees of freedom (DOFs) of the subdomain.

The velocity and acceleration fields in a subdomain are calculated by differentiating Eq. (9) with respect to time

$$\dot{\mathbf{u}}(\xi,\eta)=\mathbf{N}(\eta)\sum_{i=1}^{N}\dot{c}_i\xi^{\lambda_i}\boldsymbol{\varphi}_i \tag{11}$$

$$\ddot{\mathbf{u}}(\xi,\eta)=\mathbf{N}(\eta)\sum_{i=1}^{N}\ddot{c}_i\xi^{\lambda_i}\boldsymbol{\varphi}_i \tag{12}$$

From Eqs. (9)-(12) it is clear that the displacements, stresses, velocities and accelerations in a subdomain are all analytical with respect to the radial coordinate ξ.

3 DYNAMIC ENERGY ERROR ESTIMATOR

The energy norm of the total energy is

$$\|\mathbf{u}\|=\left(\|\mathbf{u}\|_k^2+\|\mathbf{u}\|_s^2\right)^{1/2} \tag{13}$$

where

$$\|\mathbf{u}\|_k=\left(\sum_{s=1}^{NS}\int_{V_s}\dot{\mathbf{u}}(\xi,\eta)^T\rho\dot{\mathbf{u}}(\xi,\eta)dV\right)^{1/2} \tag{14}$$

$$\|\mathbf{u}\|_s=\left(\sum_{s=1}^{NS}\int_{V_s}\boldsymbol{\sigma}(\xi,\eta)^T\mathbf{D}^{-1}\boldsymbol{\sigma}(\xi,\eta)dV\right)^{1/2} \tag{15}$$

are the energy norm of the kinetic energy and the strain energy respectively. NS is the number of subdomains.

A recovered stress field can be used to calculate the strain energy semi-analytically [8]

$$\|\mathbf{u}\|_s\approx\left(\sum_{s=1}^{NS}\sum_{i=1}^{N}\sum_{j=1}^{N}\frac{c_ic_j}{\lambda_i+\lambda_j}\int_{S_s}\boldsymbol{\sigma}_i^*(\eta)^T\mathbf{D}^{-1}\boldsymbol{\sigma}_j^*(\eta)\,|\,J\,|\,d\eta\right)^{1/2} \tag{16}$$

And the kinetic energy is [9]

$$\|\mathbf{u}\|_k=\left(\sum_{s=1}^{NS}\sum_{i=1}^{N}\sum_{j=1}^{N}\frac{\rho\dot{c}_i\dot{c}_j}{\lambda_i+\lambda_j+2}\int_{S_s}\left(\dot{\mathbf{u}}_i(\eta)\right)^T\dot{\mathbf{u}}_j(\eta)|J|d\eta\right)^{1/2} \tag{17}$$

where $\boldsymbol{\sigma}_i^*$ is the recovered stresses of ith mode at the boundary nodes, $\dot{\mathbf{u}}_i(\eta)$ is the velocity vector of ith mode along the subdomain boundary.

Substituting Eqs. (16) and (17) into Eq. (13) yields

$$\|\mathbf{u}\|=\left(\sum_{s=1}^{NS}\sum_{i=1}^{N}\sum_{j=1}^{N}\left(\frac{\rho\dot{c}_i\dot{c}_j}{\lambda_i+\lambda_j+2}\int_{S_s}\left(\dot{\mathbf{u}}_i(\eta)\right)^T\dot{\mathbf{u}}_j(\eta)|J|d\eta+\frac{c_ic_j}{\lambda_i+\lambda_j}\int_{S_s}\boldsymbol{\sigma}_i^*(\eta)^T\mathbf{D}^{-1}\boldsymbol{\sigma}_j^*(\eta)\,|\,J\,|\,d\eta\right)\right)^{1/2} \tag{18}$$

The domain energy error can be evaluated as [8]

$$\|\mathbf{e}\|\approx\left(\sum_{s=1}^{NS}\|\mathbf{e}\|_s^2\right)^{1/2} \tag{19}$$

where

$$\|\mathbf{e}\|_s\approx\sum_{i=1}^{N}\sum_{j=1}^{N}\frac{c_ic_j}{\lambda_i+\lambda_j}\int_{S_s}\mathbf{e}_{\sigma i}^*(\eta)^T\mathbf{D}^{-1}\mathbf{e}_{\sigma j}^*(\eta)\,|\,J\,|\,d\eta \tag{20}$$

is the energy error of a subdomain and

$$\mathbf{e}_{\sigma i}^{*}(\eta)=\mathbf{N}(\eta)\boldsymbol{\sigma}_{i}^{*}-\mathbf{D}(\lambda_{i}\mathbf{B}^{1}(\eta)+\mathbf{B}^{2}(\eta))\boldsymbol{\varphi}_{i} \tag{21}$$

The dynamic energy error estimator is defined as

$$\delta=\frac{\|\mathbf{e}\|}{\|\mathbf{u}\|}\times 100\% \tag{22}$$

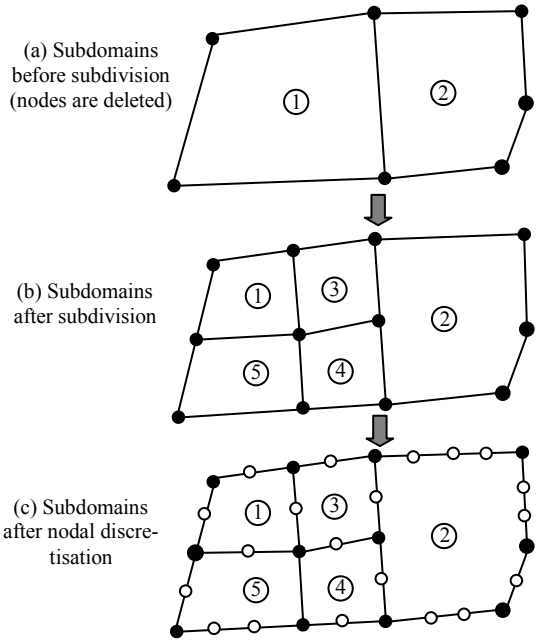

Figure 2 The remeshing procedure

4 THE ADAPTIVE PROCEDURE

4.1 Remeshing

The aim of the adaptive procedure is to make each subdomain contribute equally to the domain energy error. The average limit of the subdomain error is defined as

$$\|\mathbf{e}\|_{s}^{\lim}=\bar{\delta}\left(\frac{\|\mathbf{u}\|^{2}}{NS}\right)^{1/2} \tag{23}$$

where $\bar{\delta}$ is the target error estimator of the domain.

A parameter θ is employed to identify the subdomains that should be refined

$$\theta=\frac{\|\mathbf{e}\|_{s}}{\|\mathbf{e}\|_{s}^{\lim}} \tag{24}$$

In each time step, a very simple mesh refinement procedure applies to all subdomains with θ>1, as illustrated in Figure 2 where two subdomains in the whole domain are shown. Subdomain 1 needs to be refined and Subdomain 2 represents those connected with Subdomain 1. Figure 2a shows the two subdomains with vertices only after nodes are removed. Subdomain 1 is first subdivided into four smaller subdomains by adding a vertex at the scaling centre and a vertex at the middle point of each of the four edges, as shown in Figure 2b. The old subdomain 1 is then deleted and the topologies of the four smaller subdomains are generated. The topology of Subdomain 2 is updated with the addition of one vertex. A global seed of elemental size is then assigned to the five subdomains to generate nodes on their edges, resulting in Figure 2c for analysis.

The estimator is updated based on the new mesh until the following condition is satisfied

$$\delta<\bar{\delta} \tag{25}$$

4.2 Mesh mapping

Once a new mesh is obtained, nodal state variables, including displacement, velocity and acceleration, are transferred from the old mesh to the new one as initial conditions of the following time step. For a point or a node located at coordinates (x_0, y_0) in the new mesh after remeshing, the subdomain in the old mesh within which the point (x_0, y_0) is located is first found. The coordinates (x0, y0) are then easily transformed to SBFEM coordinates (ξ_0, η_0) by Eqs. (1) and (2) in this subdomain. Because the properties of this subdomain (eigenvalues λ_i, eigenvectors φ_i and constants c_i) are known, the displacements, velocities and accelerations at (ξ_0, η_0) in the old mesh or (x_0, y_0) in the new mesh can be calculated by Eq. (9), Eq. (11) and Eq. (12), respectively (ξ=ξ_0, η=η_0). This procedure is also very accurate because Eqs (9, 11-12) are semi-analytical. In addition, because the SBFEM discretises a domain by a few large-sized subdomains, it takes little time to locate the old subdomain for the newly-generated nodes.

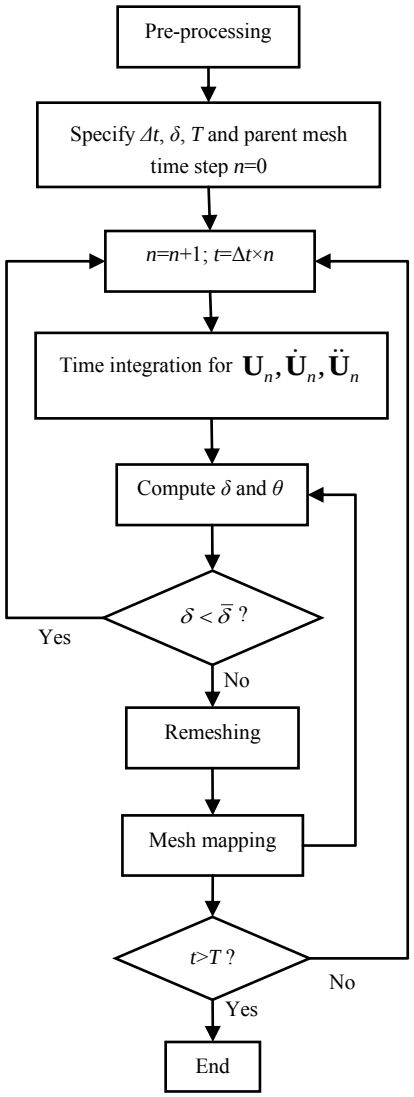

Figure 3 Flow chart of the adaptive procedure

4.3 The flow chart

Figure 3 illustrates the flow chart of the adaptive procedure. A parent mesh consisting of relatively large-sized subdomains and a target error estimator $\bar{\delta}$ are input first. At time step n, the state variables $\mathbf{U}_n, \dot{\mathbf{U}}_n, \ddot{\mathbf{U}}_n$ are solved by the Newmark integration method using the old mesh at the end of time step (n-1) and the error estimator δ is calculated. If δ exceeds the target, the adaptive procedure is triggered to identify a new mesh, starting from the parent mesh. The nodal state variables are then mapped from the old mesh to the new mesh as the initial conditions. After the state variables are solved, Eq. (25) is checked again. This iteration is repeated until an optimal adaptive mesh satisfying Eq. (25) is identified.

5 NUMERICAL EXAMPLE

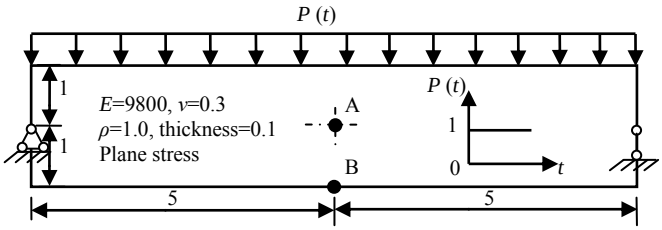

Figure 4 Dimensions of the simply-supported beam

The numerical example examined is a simply-supported beam subjected to an impact loading on the beam top face. The dimensions and material properties are shown in Figure 4. The dynamic responses in a time period of (0, 1.2s) were calculated with a constant time increment Δt=0.02s. A regular mesh (mesh 1) and an irregular mesh (mesh 2) are employed as the parent mesh, as shown in Figure 5. The target error estimator is $\bar{\delta}$ =15%. The same example was modeled in [2] using AFEM.

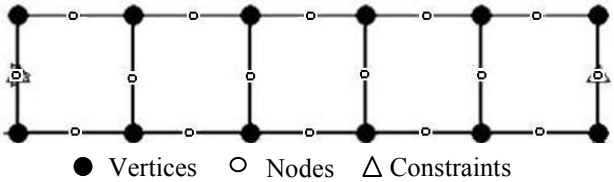

a. Mesh 1 (DOFs=56)

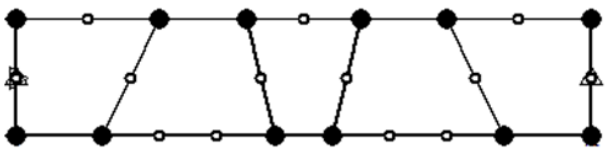

b. Mesh 2 (DOFs=50)

Figure 5 Parent meshes of the beam

Figures 6(a) and 6(b) show the horizontal stress contours and corresponding adaptive meshes at t=0.04s & 0.10s respectively. It can be observed that, with the stress wave propagation, the mesh is refined from the ends to the mid-span of the beam.

Figure 7 shows the histories of vertical displacement at point A. It can be seen that the results of non-adaptive SBFEM for both meshes gradually deviate away from the results of FEM [2] using a very fine mesh which can be considered as exact.

The results of the developed ASBFEM are better than AFEM reported in [2] and very close to FEM. Figure 8 shows the horizontal stress at point B. It can also be seen that the results of the present method agree well with FEM and better than the non-adaptive SBFEM.

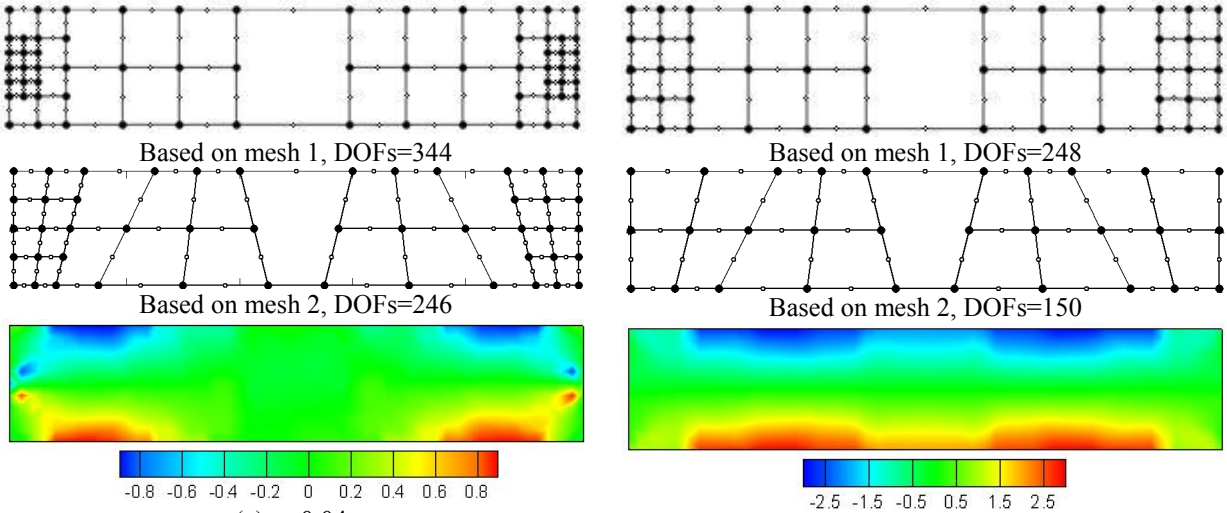

(a) t=0.04s (b) t=0.10s

Figure 6 Adaptive meshes and the horizontal stress contours

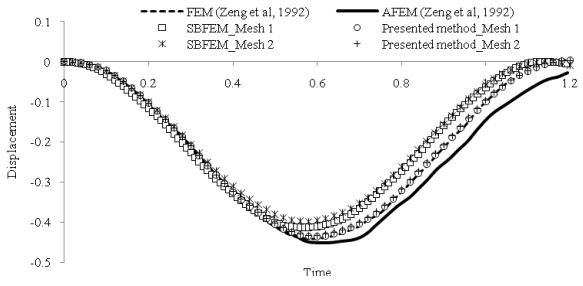

Figure 7 Histories of the vertical displacement at A

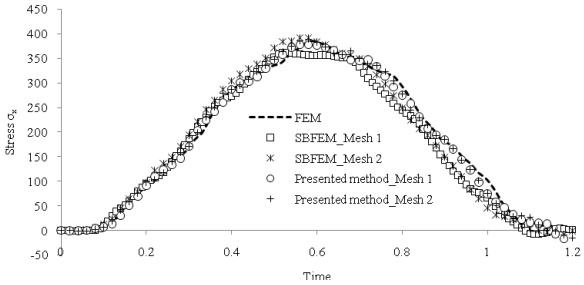

Figure 8 Histories of horizontal stress at B

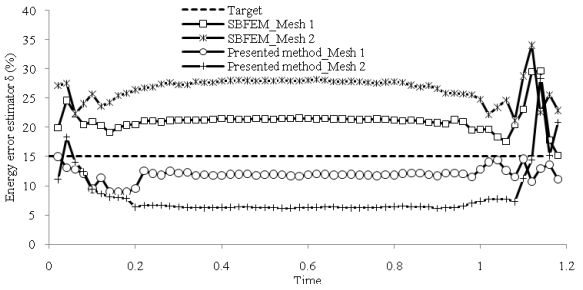

Figure 9 Histories of the energy error estimator δ

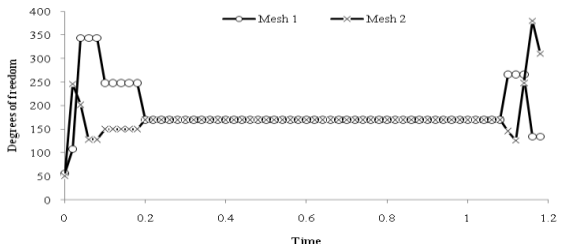

Figure 10 Histories of degrees of freedom

Figure 9 shows the histories of the energy error estimator calculated by non-adaptive SBFEM and the present method. It can be observed that the present method is able to control the estimator under the target 15% in most stages, while the estimators of the former are around 20% based on mesh 1 and 25% based on mesh 2 respectively.

Figure 10 shows the degrees of freedom used in the present ASBFEM. For this example, 150 DOFs are used in most stages while about 2,000 DOFs were used in AFEM [2].

6 CONCLUSIONS

An adaptive scaled boundary finite element method subdividing subdomains has been developed for elastodynamic problems in this study. It uses a semi-analytically integrated posteriori error estimator, and a simple and efficient mesh refinement procedure with accurate mesh mapping to adaptively identify an optimal mesh that captures stress wave propagation. An example under impact load was modelled. It has been demonstrated that the developed method is capable of computing accurate dynamic responses and effectively capturing stress wave propagation while using a fraction of degrees of freedom that are needed by adaptive finite element methods. The developed method thus provides a strong competitor in adaptive modelling of elastodynamic problems.

REFERENCES

[1] N. E. Wiberg, L. F. Zeng and X. D. Li. A postprocessed error estimate and an adaptive procedure for the semidiscrete finite element method in dynamic analysis. International Journal for Numerical Methods in Engineering, 37(21): 3585-3603, 1994.

[2] L. F. Zeng, N. E. Wiberg and L. Bernspång. An adaptive finite element procedure for 2D dynamic transient analysis using direct integration. International Journal for Numerical Methods in Engineering, 34(3): 997-1014, 1992.

[3] J. P. Wolf and C. M. Song. The scaled boundary finite-element method-a primer: derivations. Computers and Structures, 78(1-3): 191-210, 2000.

[4] C. M. Song and J. P. Wolf. The scaled boundary finite-element method-a primer: solution procedures. Computers and Structures, 78(1-3): 211-225, 2000.

[5] E. T. Ooi and Z. J. Yang. Modelling dynamic crack propagation using scaled boundary finite element method. International Journal for Numerical Methods in Engineering, in press.

[6] N. M. Newmark. A method of computation for structural dynamics. ASCE Journal of the Engineering Mechanics Division, 85: 67-94, 1959.

[7] A. J. Deeks and J. P. Wolf. A virtual work derivation of the scaled boundary finite-element method for elastostatics. Computational Mechanics, 28: 489-504, 2002.

[8] A. J. Deeks and J. P. Wolf. Stress recovery and error estimation for the scaled boundary finite-element method. International Journal for Numerical Methods in Engineering, 54(4): 557-583, 2002.

[9] Z. J. Yang, A. H. Zhang, G. H. Liu and E. T. Ooi. An *h*-hierarchical adaptive scaled boundary finite element method for elastodynamics, *Computers and Structures*, under review.